Dense Neural Network for Classification of Seafloor Sediment using Backscatter Mosaic Feature

Khomsin[1] , *Danar* Guruh Pratomo[1], *Muhammad* Aldila Syariz[1], *Irena* Hana Hariyanto[1], *Hessi* Candra Harisa[1]
[1]Department of Geomatics Engineering, Sepuluh Nopember Institute of Technology, Surabaya, Indonesia 60111

Abstract. Water transportation plays a vital role in global economic activities, facilitating more than 85% of international trade and serving as a cost-effective and essential means to fulfill the demand for goods and services. Similarly, the Benoa Port, situated in the southern part of Denpasar City, operates in the same manner. By utilizing Multibeam Echo Sounder (MBES) backscatter data, backscatter mosaics can be generated to identify various seafloor sediment types, which consist of rock fragments, minerals, and organic materials. The characteristics of these sediments, such as grain size, density, composition, and others, can be observed. To improve the classification of sediments, the integration of backscatter data and backscatter features, such as ASM (Angular Second Moment), Energy, Contrast, and Correlation, can be employed. Supervised classification models like Dense Neural Network (DNN) can be utilized to accurately determine the types of seafloor sediments. The application of DNN modeling resulted in a training accuracy rate of 88% and a testing accuracy rate of 100%. The accuracy results delineated six distinct sediment types. Notably, sandy silt exhibited the highest distribution, accounting for 49.30%, whereas soft clayey silt registered the lowest distribution at 0.53%, as determined by their respective spatial prevalence.

1 Introduction

Sea transportation is one of the potentials that Indonesia possesses in the maritime sector [1]. The ocean serves as a vital transportation route for both passenger and cargo traffic within Indonesia, connecting islands, countries, and even continents [2]. Water transport is a crucial component of global economic exchanges, responsible for more than 85% of international trade and serving as the most affordable and indispensable means to meet the demand for goods and services [3]. The same is the case with the Benoa Port, Bali. The port is used for ship loading for domestic and international trade, while other parts are used for cruise ships. In order to guarantee safety and comfort during sea transportation, it is essential to obtain information about seafloor conditions through the implementation of hydrographic surveys [1]. A Multibeam Echosounder is one instrument that can be used for hydrographic surveys. The Multibeam survey technique was developed in the 1960s and is still used in marine resource surveys, marine engineering building, and marine science research [4]. Due to the progress in Multibeam Echosounder (MBES) technology, it is now possible to obtain comprehensive data sets of the physical structure across extensive areas of the seafloor [5]. A Multibeam echosounder exploits the acoustic waves emitted to the ocean floor through a transducer and records the reflections of those waves using a receiver [6]. The intensity of the reflected acoustic wave depends on the material of the seafloor, such as sediments, rock, coral reef, and seafloor roughness [7]. In hydrographic survey measurements using multibeam echosounders, three types of data are obtained: depth data, backscatter data, and water column data [8].

* Corresponding author: khomsin@geodesy.its.ac.id

Seafloor sediment classification involves the recognition, mapping, and analysis of the physical attributes, distribution, and ecological condition of different entities using acoustic or optical techniques, supplemented by various detection methods [18]. To determine the classification of seafloor sediment types using backscatter, it can be based on the amplitude of the returning sound waves, where strong signals indicate a hard seafloor surface (rocks, gravel), while weak signals indicate a smoother seafloor (silt, clay) [19]. To expand the research on the potential of MBES in classifying seafloor sediments, a new method is proposed that integrates backscatter mosaic data and backscatter mosaic features to improve the results of seafloor sediment classification.

Backscatter mosaic features are obtained from the processed backscatter mosaic data using the gray level co-occurrence matrix (GLCM) method. GLCM is a widely used technique for extracting texture-based features, as it calculates the second-order statistics of images to determine the textural correlation between pixels [20]. In backscatter mosaics, there is additional information, such as texture information, that not only reflects the characteristics of the water bottom surface and its relationship with the surrounding environment but also provides information about the macro and microstructures within the water bottom [21, 22]. There are four features used: Angular Second Moment (ASM), Energy, Contrast, and Correlation. Each feature provides different information about the structure and texture of sediments, such as roughness, regularity, and variation. These features also help differentiate between different types of sediments, such as sand, mud, or rock [23]. To determine the classification of seafloor sediments, one example of a supervised classification model that can be used is the Neural Network [24]. Dense Neural Network (DNN) is one of the simplest forms of Neural Network methods [25]. DNN for sediment classification has several advantages over manual methods, including speed and efficiency, objectivity, and flexibility. The accuracy of seafloor sediment classification is determined by several factors. In addition to the data used, the classification results also depend on the utilization of the classification model [24].

Based on the background discussed, this research aims to determine the appropriate design of a DNN model to achieve the classification of sediment types and their distribution using processed backscatter mosaic data and backscatter mosaic features around Benoa Port, Bali.

2 Methods

The research location is in Benoa Port, Denpasar City, Bali (see Figure 1). The establishment is situated in close proximity to well-known destinations such as Nusa Dua, Sanur, Kuta, and Denpasar. Geographically, Benoa Port is located at 8°44’45.76” South Latitude and 115°12’40.61” East Longitude. Benoa Port is accessed through a navigational channel spanning 2 nautical miles and is equipped with two berths, namely the East Berths and the South Berths, both measuring 290 meters in length. The South Berth, serving as an alternative, has a length of 206 meters.

2.1 Bathymetric Data

This study employs the MBES as the instrument for data acquisition. A component resulting from the bathymetric survey carried out using the R2Sonic 2020 MBES is the raw data utilized in this research, identified by the *.SBD extension. The bathymetric survey was conducted on January 31, 2022. The data in this research used multi-frequency data divided into 5 frequencies: 170 kHz, 220 kHz, 270 kHz, 350 kHz and 400 kHz. The research area includes the port area to the east and south, as well as the area around the port entrance.

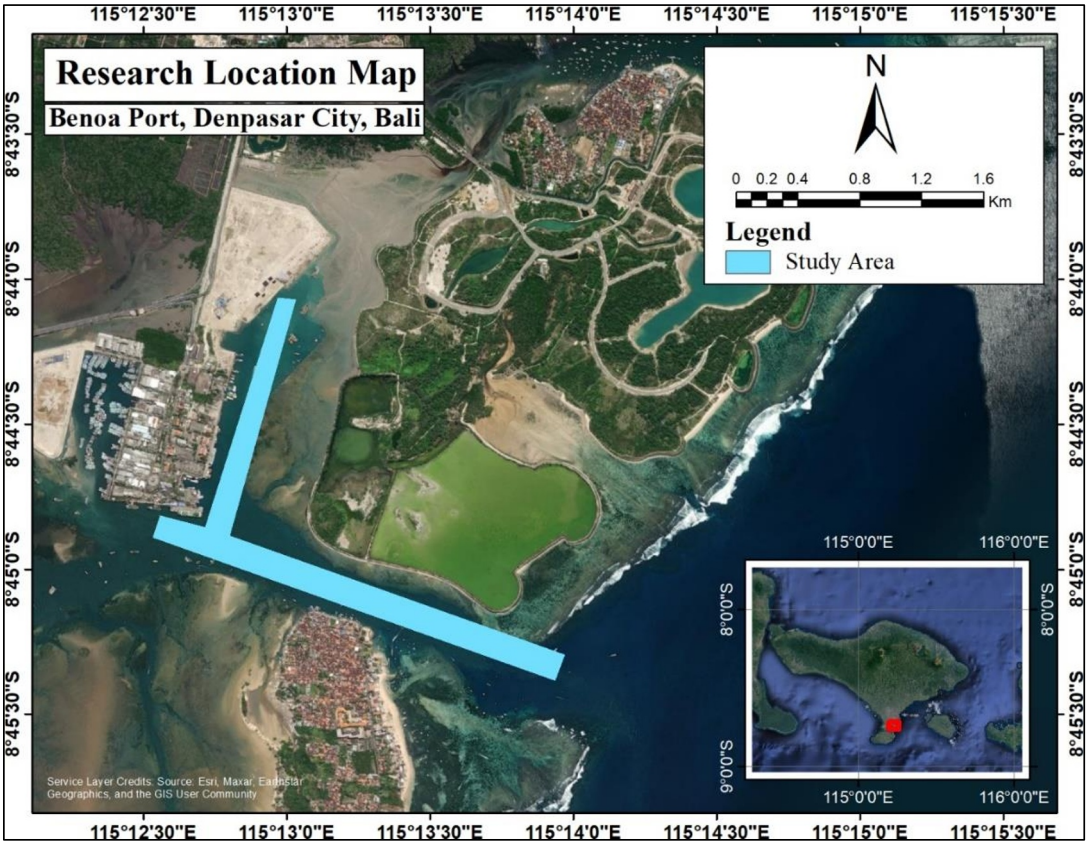

Fig. 1. Study Area

2.2 Sediment Sample

In this research, 12 sediment sample points were used as primary data. There are six types of sediments distributed among the 12 sediment sample points. The sediment sample data can be seen in Table 1, and their distribution can be observed in Figure 2.

Table 1. Sediment Sample

Point	Sediment Type
PT1	Silty gravel with coral
PT2	Silty gravel with coral
PT3	Silty gravel with coral
PT4	Silty gravel with coral
PT5	Sandy silt
PT6	Sandy silt
PT7	Silty sand
PT8	Silty sand
PT9	Silty sand
PT10	Gravelly coral sand with silty gravel
PT11	Soft clayey silt

PT12	Gravelly sand

Fig. 2. Distribution of Sediment Sample Location in the Research Area

2.3 Data Processing

2.3.1 Processing Raw MBES Data

The raw MBES data is multi-frequency data, so it is necessary to separate the frequencies into five frequencies using NaviEdit, followed by depth correction. The corrected data is then modeled with a Digital Terrain Model (DTM) using NaviModel for easier filtering. The purpose of filtering the data is to remove noise or incorrect depth values. After the filtering stage is completed, a thorough inspection is conducted to ensure the data's quality and accuracy. The clean filtered data is exported in *.gsf format, and then the mosaic process is applied to generate the backscatter mosaic using FMGT software.

2.3.2 Extraction of Backscatter Mosaic Features

The raster data from the backscatter mosaic processing is extracted using GLCM method with SNAP software, resulting in raster data of four backscatter mosaic features: ASM, contrast, correlation, and energy. The subsequent step involves extracting the intensity values from both the backscatter mosaic raster data and the backscatter mosaic feature raster data by utilizing sediment sample data.

2.3.3 DNN Classification

The intensity values assigned to each sediment point are partitioned into two subsets: 70% for training purposes and 30% for testing. Subsequently, the initial DNN model undergoes training, yielding a trained DNN model that is subsequently tested to assess its accuracy. The activation functions employed in the DNN model include ReLU and Sigmoid. The classification

process is performed using data from the DNN model with the best accuracy. Raster data is acquired from both the backscatter mosaic and the backscatter feature mosaic for each specific point. Subsequently, this obtained data is utilized in the classification and mapping processes, aiming to generate sediment classification and distribution.

3 Result and Discussion

3.1 Training Data and Testing Data

Data training is the data used to train a model using the DNN method, while data testing is the data used to make predictions based on the model that has been trained using the training data. There are 12 sediment points scattered along the MBES measurement track. Out of these twelve sediment points, nine sediment points are allocated for training, and three sediment points are allocated for testing. The division of the training data and testing data can be seen in Table 2 and Table 3.

Table 2. Training Data

Point	Sediment Type
PT1	Silty gravel with coral
PT2	Silty gravel with coral
PT3	Silty gravel with coral
PT5	Sandy silt
PT7	Silty sand
PT9	Silty sand
PT10	Gravelly coral sand with silty gravel
PT11	Soft clayey silt
PT12	Gravelly sand

Table 3. Testing data

Point	Sediment Type
PT4	Silty gravel with coral
PT6	Sandy silt
PT8	Silty sand

This data division is done randomly and repeatedly to obtain the best model results. However, for the testing data, there is a specific condition that selects sediment types that have positions in more than 1 point. This means that sediment points PT10, PT11, and PT12 are not used for testing data because they only have sediment types in 1 point.

3.2 Dense Neural Network Model

In the DNN method, each neuron in a particular layer is connected to every neuron in the next layer. The construction of the Dense Neural Network model is done using the Python programming language, processed online using the cloud platform provided by Google called Google Colab. To implement DNN with Python, the deep learning libraries TensorFlow and Keras are used. DNN model consists of three fully-connected layers: the input layer, hidden layer, and output layer. To obtain the best-performing model, the author created six different models as follows.

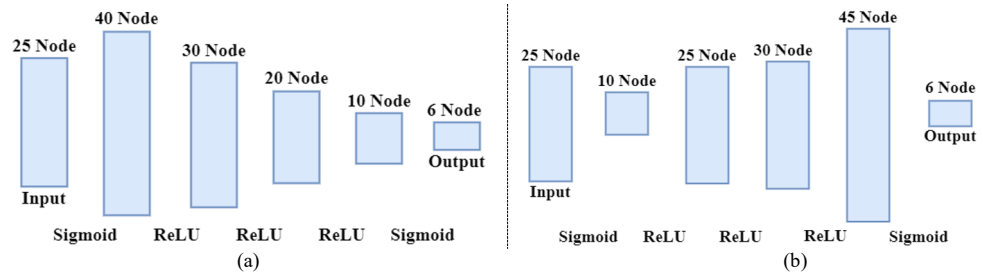

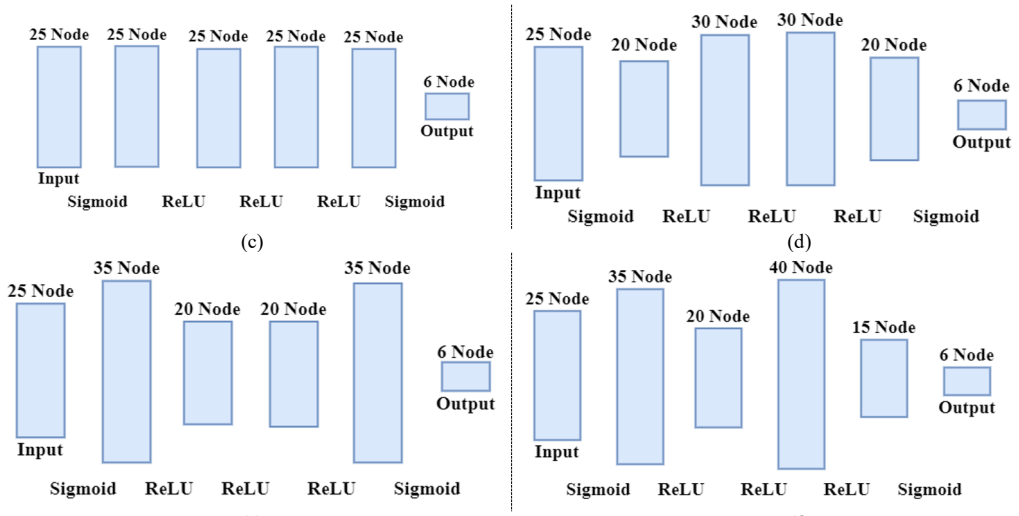

Fig. 3. DNN Model (a) DNN Model 1 (b) DNN Model 2 (c) DNN Model 3 (d) DNN Model 4 (e) DNN Model 5 (f) DNN Model 6

Configuring the DNN model requires the explicit specification of multiple parameters, encompassing the quantity of neurons in the input layer, the determination of hidden layers and their respective neuron quantities, the configuration of the output layer's neuron count, the chosen activation function, and adjustments for both epoch and batch size settings. In the DNN model, hyperparameters such as the optimizer, loss function, and metrics are used. The optimizer utilizes Adaptive Moment Estimation (Adam), the loss function is categorical crossentropy, and the metrics employed are accuracy.

In Figure 3, each model has a different number of neurons/nodes in the input layer and output layer. This is because obtaining a good model requires conducting numerous experiments, and from these experiments, the best results can be obtained. The difference in the number of nodes in each model is based on the total number of parameters. Total parameters refer to the sum of all parameters generated in each layer. In this case, each model has a total number of parameters that are not significantly different. DNN Model 1 has a total of 3,166 parameters, DNN Model 2 has 2,986, DNN Model 3 has 2,756, DNN Model 4 has 2,826, DNN Model 5 has 3,001, and DNN Model 6 has 3,181. Creating these six different models aims to facilitate finding the best accuracy value.

3.3 Model Evaluation Results

The evaluation results of the model are the outcome of modeling accuracy in training the model, which will be further used for classification purposes. These results include accuracy values for both training and testing. The higher the accuracy value, the better the model created. It is important to have good accuracy results for both training and testing. If the training accuracy is high but the testing accuracy is low, the DNN model will experience underfitting. Conversely, if the training accuracy is low but the testing accuracy is high, the DNN model will experience overfitting. Underfitting and overfitting accuracy results can hinder the ability of the DNN model to generalize well on data. Therefore, it is crucial to find a balanced or not-too-distant value to obtain accurate classification results (see Table 4).

Table 4. DNN Model Accuracy

DNN Model	Epoch	Training Accuracy	Testing Accuracy
DNN Model 1	200	88%	66%
DNN Model 2		77%	66%
DNN Model 3		88%	33%
DNN Model 4		88%	66%
DNN Model 5		88%	100%
DNN Model 6		88%	33%

Based on the accuracy results, DNN Model 1, DNN Model 3, DNN Model 4, DNN Model 5, and DNN Model 6 have the same training accuracy of 88%. However, in terms of testing accuracy, DNN Model 5 has the highest accuracy of 100%.

Therefore, this study will use DNN Model 5 as the DNN model for the classification process. The overall classification accuracy of seafloor sediments can be significantly improved using a DNN classification model with different weights [24].

3.4 Classification of Seafloor Sediments

Based on the sediment sample data, which consists of 12 sediment samples, it is indicated that there are 6 types of sediments. The classification of seafloor sediments, which is the result of processing the DNN model, refers to the sediment sample points. From the classification processing, values ranging from 1 to 6 are obtained for each point of the extracted raster values previously conducted. Thus, from the classification results, a sediment distribution map can be created for Benoa Port (see Figure 3).

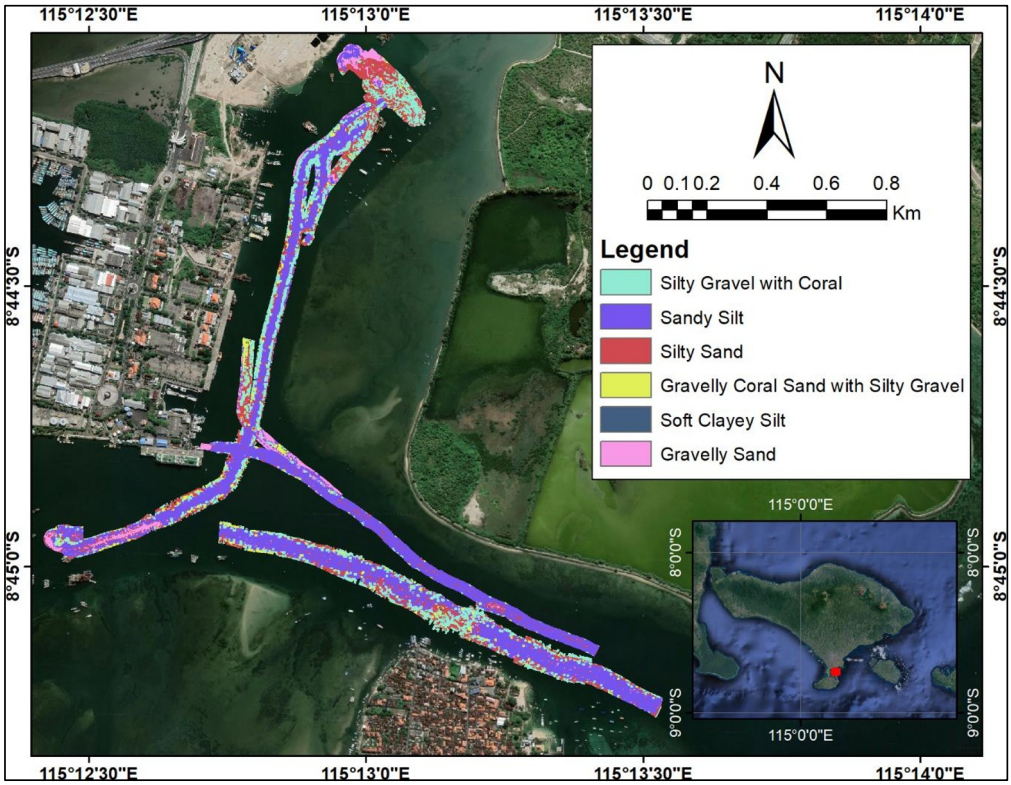

Fig. 3. Sediment Distribution Map

In Figure 3, it can be observed that the sediment type "sandy silt" has the largest distribution. When viewed in percentages, the "sandy silt" sediment type has the highest percentage, which is 49.30%. This is followed by silty gravel with coral at 22.32%, silty sand at 17.49%, gravelly sand at 5.80%, gravelly coral sand with silty gravel at 4.56%, and the sediment type soft clayey silt has the smallest percentage, which is 0.53%.

The distribution of seafloor sediment types in Figure 3 exhibits a pattern where the sandy silt is spread in the middle of the track, while other sediment types are spread along the edges of the track. This pattern can be influenced by various factors, such as limited data variability, insufficient data, and model complexity. To ensure the correct sediment types, validation can be performed by comparing the sediment types from the sediment samples with the processed results. From this validation, it can be determined which points match the sediment types in the sediment samples and which points do not match (see Table 5).

Table 5. Comparison between sediment types from sediment samples and from DNN processing

Point	Sediment Type	
	Sediment Sample	**DNN Processing**
PT1	Silty gravel with coral	Silty gravel with coral
PT2	Silty gravel with coral	Silty gravel with coral
PT3	Silty gravel with coral	Silty gravel with coral
PT4	Silty gravel with coral	Silty gravel with coral
PT5	Sandy silt	Sandy silt
PT6	Sandy silt	Gravelly sand
PT7	Silty sand	Sandy silt
PT8	Silty sand	Silty sand
PT9	Silty sand	Silty sand
PT10	Gravelly coral sand with silty gravel	Gravelly coral sand with silty gravel
PT11	Soft clayey silt	Sandy silt
PT12	Gravelly sand	Gravelly sand

The comparison between the sediment types from the sediment samples and the sediment types from the DNN processing yielded identical results except for three sediment points, namely PT6, PT7, and PT11. The discrepancy in sediment types may be attributed to limitations in the training data and errors in the model structure or model parameters. Therefore, during the DNN model processing, it is crucial to ensure that the training data and model are accurately aligned to achieve accurate sediment classification.

4 Conclusion

Based on the conducted research, it can be concluded that the best-performing DNN model achieved a training accuracy of 88% and a testing accuracy of 100%. The classification results for the seafloor sediment types in Benoa Port revealed six categories: silty gravel with coral, sandy silt, silty sand, gravelly coral sand with silty gravel, soft clayey silt, and gravelly sand. The most dominant sediment type is sandy silt with a percentage of 49.30%, followed by silty gravel with coral at 22.32%, silty sand at 17.49%, gravelly sand at 5.80%, gravelly coral sand with silty gravel at 4.56%, and the sediment type soft clayey silt has the smallest percentage, which is 0.53%. With this research expected to provide significant benefits in a variety of contexts, from marine science to natural resource management and marine technology. In the classification of types of seafloor sediment, this research is also expected to have better accuracy compared to other methods.

The author extends gratitude to PT. Pelabuhan Indonesia (Persero) Regional 3 for supplying the bathymetric and soil dataset employed in this research, and acknowledges EIVA for the provision of the EIVA NaviEdit and NaviModel software.

References

1. G. Nikawanti and R. Aca, “Ecoliteracy: Membangun Ketahanan Pangan dari Kekayaan Maritim Indonesia,” *Jurnal Kemaritiman: Indonesian Journal of Maritime*, vol. 2, no. 2, 2021.
2. Khomsin, D. G. Pratomo, and I. Saputro, “Comparative analysis of singlebeam and multibeam echosounder bathymetric data,” *IOP Conf Ser Mater Sci Eng*, vol. 1052, no. 1, p. 012015, Jan. 2021, doi: 10.1088/1757-899x/1052/1/012015.
3. F. Nicolae, M. Bucur, and A. Cotorcea, “Port Performance Evaluation. Case study: Ports in the Black Sea Basin,” *IOP Conf Ser Earth Environ Sci*, vol. 172, no. 1, Jul. 2018, doi: 10.1088/1755-1315/172/1/012004.
4. Q. Tang, X. Liu, X. Ji, J. Li, Y. Chen, and B. Lu, “Using Seabed Acoustic Imagery to Characterize and Classify Seabed Sediment Types in the Pockmark Area of the North Yellow Sea, China,” *Applied Acoustics*, vol. 174, Mar. 2021, doi: 10.1016/j.apacoust.2020.107748.
5. X. Ji, B. Yang, and Q. Tang, “Seabed Sediment Classification using Multibeam Backscatter Data based on the Selecting Optimal Random Forest Model,” *Applied Acoustics*, vol. 167, Oct. 2020, doi: 10.1016/j.apacoust.2020.107387.
6. R. Nitriansyah and B. K. Cahyono, “Seabed Classification Using Multibeam Echosounder Measurement Data,” *IOP Conf Ser Earth Environ Sci*, vol. 1039, no. 1, 2022, doi: 10.1088/1755-1315/1039/1/012045.
7. Subarsyah and L. Arifin, “Seabed Characterization through Image Processing of Side Scan Sonar Case Study: Bontang and Batam,” *Bulletin of the Marine Geology*, vol. 34, no. 1, pp. 37–50, 2019.
8. P. Porskamp, A. C. G. Schimel, M. Young, A. Rattray, Y. Ladroit, and D. Ierodiaconou, “Integrating Multibeam Echosounder Water-column Data into Benthic Habitat Mapping,” *Limnol Oceanogr*, vol. 67, no. 8, pp. 1701–1713, Aug. 2022, doi: 10.1002/lno.12160.

9. G. A. Rocha, A. C. Bastos, G. M. Amado-Filho, G. C. Boni, R. L. Moura, and N. Oliveira, "Heterogeneity of rhodolith beds expressed in backscatter data," *Mar Geol*, vol. 423, May 2020, doi: 10.1016/j.margeo.2020.106136.
10. T. Zhao, G. M. Gavazzi, S. Lazendić, Y. Zhao, and A. Pižurica, "Acoustic Seafloor Classification using the Weyl Transform of Multibeam Echosounder Backscatter Mosaic," *Remote Sens (Basel)*, vol. 13, no. 9, 2021, doi: 10.3390/rs13091760.
11. J. Wan *et al.*, "MBES Seabed Sediment Classification Based on a Decision Fusion Method Using Deep Learning Model," *Remote Sens (Basel)*, vol. 14, no. 15, Aug. 2022, doi: 10.3390/rs14153708.
12. Khomsin, Mukhtasor, D. G. Pratomo, and Suntoyo, "The Development of Seabed Sediment Mapping Methods: The Opportunity Application in the Coastal Waters," *IOP Conf Ser Earth Environ Sci*, vol. 731, no. 1, Apr. 2021, doi: 10.1088/1755-1315/731/1/012039.
13. B. S. Halpern *et al.*, "Recent Pace of Change in Human Impact on the World's Ocean," *Sci Rep*, vol. 9, no. 1, Dec. 2019, doi: 10.1038/s41598-019-47201-9.
14. C. C. O'Hara, M. Frazier, and B. S. Halpern, "At-risk Marine Biodiversity Faces Extensive, Expanding, and Intensifying Human Impacts," *Science (1979)*, vol. 372, no. 6537, pp. 84–87, Apr. 2021, doi: 10.1126/science.abe6731.
15. G. Epstein, J. J. Middelburg, J. P. Hawkins, C. R. Norris, and C. M. Roberts, "The Impact of Mobile Demersal Fishing on Carbon Storage in Seabed Sediments," *Global Change Biology*, vol. 28, no. 9. John Wiley and Sons Inc, pp. 2875–2894, May 01, 2022. doi: 10.1111/gcb.16105.
16. R. Awal, P. Sapkota, S. Chitrakar, B. S. Thapa, H. P. Neopane, and B. Thapa, "A General Review on Methods of Sediments Sampling and Mineral Content Analysis," *IOP Conference Series: Journal of Physics*, vol. 1266, no. 1, 2019, doi: 10.1088/1742-6596/1266/1/012005.
17. R. A. Rachman and M. Wibowo, "Study of Sea Bottom Sediment Characteristic to Support Patimban Port Development Plan," *Jurnal Geologi Kelautan*, vol. 17, no. 2, 2019, doi: http://dx.doi.org/10.32693/jgk.17.2.2019.592.
18. X. Cui, F. Yang, X. Wang, B. Ai, Y. Luo, and D. Ma, "Deep Learning Model for Seabed Sediment Classification Based on Fuzzy Ranking Feature Optimization," *Mar Geol*, vol. 432, Feb. 2021, doi: 10.1016/j.margeo.2020.106390.
19. P. Adi, H. M. Manik, and S. Pujiyati, "Integrasi Data Multibeam Batimetri dan Mosaik Backscatter untuk Klasifikasi Tipe Sedimen," *Jurnal Teknologi Perikanan dan Kelautan*, vol. 7, no. 1, pp. 77–84, 2016, doi: https://doi.org/10.24319/jtpk.7.77-84.
20. Ş. Öztürk and B. Akdemir, "Application of Feature Extraction and Classification Methods for Histopathological Image using GLCM, LBP, LBGLCM, GLRLM and SFTA," *Procedia Comput Sci*, vol. 132, pp. 40–46, 2018, doi: 10.1016/j.procs.2018.05.057.
21. R. M. Haralick, I. Dinstein, and K. Shanmugam, "Textural Features for Image Classification," *IEEE Trans Syst Man Cybern*, vol. SMC-3, no. 6, pp. 610–621, 1973, doi: 10.1109/TSMC.1973.4309314.
22. W. Sun, A. Z. Kolappal, and P. Gong, "Two Computation Methods for Detecting Anisotropy in Image Texture,"*Geographic Information Sciences*, vol. 11, no. 2, pp. 87–96, 2005, doi: 10.1080/10824000509480604.
23. S. A. Samsudin and R. C. Hasan, "Assessment of Multibeam Backscatter Texture Analysis for Seafloor Sediment Classification," in *International Archives of the Photogrammetry, Remote Sensing and Spatial Information Sciences - ISPRS Archives*, International Society for Photogrammetry and Remote Sensing, Sep. 2013, pp. 177–183. doi: 10.5194/isprs-archives-XLII-4-W5-177-2017.
24. Z. Zhu, X. Cui, K. Zhang, B. Ai, B. Shi, and F. Yang, "DNN-based Seabed Classification using Differently Weighted MBES Multifeatures," *Mar Geol*, vol. 438, Aug. 2021, doi: 10.1016/j.margeo.2021.106519.
25. F. Amherd and E. Rodriguez, "Heatmap-based Object Detection and Tracking with a Fully Convolutional Neural Network," Jan. 2021, [Online]. Available: http://arxiv.org/abs/2101.03541